Improved Mapping Functions for Atmospheric Refraction Correction in SLR

V. B. Mendes

Laboratório de Tectonofísica e Tectónica Experimental and Departamento de Matemática, Faculdade de Ciências da Universidade de Lisboa, 1749-016 Lisboa, Portugal

G. Prates

Escola Superior de Tecnologia da Universidade do Algarve, Faro, Portugal

E. C. Pavlis

Joint Center for Earth Systems Technology, University of Maryland Baltimore County and NASA Goddard 926, Greenbelt, MD 20771, USA

D. E. Pavlis

Raytheon Information Technology and Science Services and NASA Goddard 926, Greenbelt, MD 20771, USA

R. B. Langley

Geodetic Research Laboratory, Department of Geodesy and Geomatics Engineering, University of New Brunswick, Fredericton, N.B. E3B 5A3, Canada

Abstract. We present two new mapping functions (MFs) to model the elevation angle dependence of the atmospheric delay for satellite laser ranging (SLR) data analysis. The new MFs were derived from ray tracing through a set of data from 180 radiosonde stations globally distributed, for the year 1999, and are valid for elevation angles above 3°. When compared against ray tracing of two independent years of radiosonde data (1997-1998) for the same set of stations, our MFs reveal submillimetre accuracy for elevation angles above 10°, representing a significant improvement over other MFs, and is confirmed in improved solutions of LAGEOS and LAGEOS 2 data analysis.

1. Introduction

The main accuracy-limiting factor in modern space geodetic techniques, such as the Global Positioning System (GPS), very long baseline interferometry (VLBI), and satellite laser ranging (SLR), is atmospheric refraction.

The atmospheric refraction modeling at radio wavelengths has improved significantly in the last decade and high accuracy models and data processing strategies are available (see *Mendes* [1999] for a review). Such progress contrasts sharply with the situation at optical wavelengths, where most data analysis is still being performed with the Marini-Murray refraction model [*Marini and Murray,* 1973], developed in the early 1970s. Better atmospheric refraction modeling is of great importance in reducing the error budget in SLR measurements in high-precision geodetic and geophysical applications, such as the study of spatial and temporal variations in the Earth's gravity field, the monitoring of vertical crustal motion, and the prospect of a more robust combination of solutions from different space techniques.

Paper number .
0094-8276/02/$5.00

2. Atmospheric Refraction

For modeling purposes, the atmospheric refraction can be explicitly written as the contribution of a hydrostatic and a wet component, each one consisting of the product of the delay experienced in the zenith direction and a mapping function (MF) that models the elevation angle dependence of atmospheric refraction (e.g. *Mendes* [1999]):

$$d_{atm} = d_h^z \cdot m_h(\epsilon) + d_w^z \cdot m_w(\epsilon), \tag{1}$$

where d_{atm} is the atmospheric refraction at a given (unrefracted) elevation angle ϵ, d_h^z and d_w^z are the hydrostatic and wet zenith delays (ZDs), and $m_h(\epsilon)$ and $m_w(\epsilon)$ are the hydrostatic and wet MFs, respectively.

Due to the small contribution of water vapor to atmospheric refraction at visible wavelengths, we can consider a single MF for SLR. In this case, we have:

$$d_{atm} = d_{atm}^z \cdot m(\epsilon), \tag{2}$$

where d_{atm}^z is the total zenith propagation delay and $m(\epsilon)$ the (total) MF.

The one-way propagation delay experienced by a laser signal in the zenith direction is defined as

$$d_{atm}^z = 10^{-6} \int_{r_s}^{r_a} N \, dz, \tag{3}$$

where N is the group refractivity, r_s is the geocentric radius of the laser station, r_a is the geocentric radius of the top of the neutral atmosphere, and dz has length units.

Marini and Murray [1973] developed a full model for atmospheric refraction modeling that is currently recommended by the IERS Conventions [*McCarthy,* 1996]. For this model, valid for elevation angles greater than 10°, there is no clear separation between the ZD and the MF.

Saastamoinen [1973] also developed a full model, which allows easy separation of the ZD model and MF, but again is only valid for elevation angles above 10°.

More recently, *Yan and Wang* [1999] presented a new MF based on the expansion of the complementary error function.

3. Mapping Function Development

The functional model of our new MFs is based on a truncated form of the continued fraction in terms of $1/\sin(\epsilon)$ [*Marini,* 1972], normalized to unity at the zenith:

$$m(\epsilon) = \frac{1 + \frac{a_1}{1+\frac{a_2}{1+a_3}}}{\sin\epsilon + \frac{a_1}{\sin\epsilon+\frac{a_2}{\sin\epsilon+a_3}}}. \qquad (4)$$

Such a functional model has already been used as the basis of mapping functions for radio wavelengths with acknowledged success (e.g. *Niell* [1996]).

The development of the new functions is based on ray tracing (for details on this procedure see, e.g., *Mendes* [1999]) through one full year (1999) of radiosonde data from 180 stations, globally distributed, with a variable number of balloon launches per day. For one of the stations (Diego Garcia, British Indian Ocean Territory) we have used data from 1998, due to lack of data in 1999. The radiosonde data consists of height profiles of pressure, temperature and relative humidity. The heights for all levels were calculated from reported temperature and pressure using the hypsometric equation [*Dutton,* 1986]. As recommended by the International Association of Geodesy [*IUGG,* 1999], the group refractivity was computed using the procedures described in *Ciddor* [1996] and *Ciddor and Hill* [1999].

The ray tracing procedure was performed at 22 elevation angles (3°, 4°, 5°, 6°, 8°, 10°, and every 5°thereafter), and tuned for the most-used SLR wavelength (λ=532 nm). For each radiosonde launch we have determined (in a least-squares sense) the coefficients a_i (i = 1,2,3) in Equation (4). All coefficients deviating significantly from the average (using a 4-sigma threshold) were considered outliers and removed, resulting in acceptance of a total of 87,766 sets of coefficients. After a preliminary analysis of the dependence of the coefficients on the different site locations and meteorological data, we adopted two different parameterisations and the coefficients in Equation (4) were subsequently written as functions of the selected parameters.

One parameterisation of the MF (**FCULa**) requires both site location and meteorological (surface temperature) data; the coefficients of the MF have the following mathematical formulation:

$$a_i = a_{i0} + a_{i1}t_s + a_{i2}\cos\varphi + a_{i3}H, (i = 1, 2, 3) \qquad (5)$$

where t_s is the temperature at the station in Celsius degrees, φ is the station latitude, and H is the orthometric height of the station, in metres.

The second MF (**FCULb**) does not depend on any meteorological data and follows the reasoning behind the model developed by *Niell* [1996] for radio wavelengths. For this function, the coefficients have the following form:

$$a_i = a_{i0} + (a_{i1} + a_{i2}\varphi_d^2)\cos\left(\frac{2\pi}{365.25}(doy - 28)\right) + a_{i3}H + a_{i4}\cos\varphi, (i = 1, 2, 3) \qquad (6)$$

where φ_d is the latitude of the station, in degrees, and *doy* is the decimal day of year (UTC days since the beginning of the year). We have adopted the value of the phase of 28 days obtained by *Niell* [1996], but in our approach simple functions replace the interpolation schemes for day of year and latitude used by Niell. The different coefficients for these functions are listed in Table 1.

The advantages of the new MFs are obvious. They represent simpler expressions than those used by the Marini-Murray model and allow the use of better ZD models; their parameterisation depends on a readily available meteorological parameter value (the surface temperature at the site) and site location information, or, alternatively and with a small degradation in performance, site location information and day of year (the prediction of the zenith delay requires, however, accurate measurements of surface pressure). Finally, these new MFs permit the analysis of data taken at low elevation angles and are more accurate than other mapping functions at all elevation angles.

4. Model Assessment

The following analysis is based on the overall performance of the MFs, when tested against 2 years of radiosonde data (1997−1998), for the same set of 180 stations, for a total of over 163,000 benchmark values.

In general, FCULa performs better than FCULb (at the millimetre level), with the largest differences between the two functions found in Asia and the southwest Pacific (Figure 1 shows the global performance of FCULa, for $\epsilon = 10°$). As presented in Table 2 (all statistics given in the tables and elsewhere in the paper are based on the differences between the model predictions and the ray-traced values, i.e., model minus trace), the r.m.s. for FCULa is about 1 mm, 4 mm and 16 mm, at elevation angles of 15°, 10°, and 6°, respectively. This table shows both the two-year-averaged values for the mean, standard deviation (std), and r.m.s. for the total number of differences and maximum (max) r.m.s. value obtained at each radiosonde station, for the same period.

The performance of FCULa degrades from low to high latitudes, mainly due to the higher seasonal variation of the surface temperature. At 6°elevation angle, for example, the overall r.m.s. increases from ∼1 cm, for the latitude range 15°S – 15°N, to more than 2.5 cm, for stations at latitudes greater than 75°(absolute values). There are no significant differences in performance in the different hemispheres.

Comparison of the new mapping functions against those of *Saastamoinen* [1973] and *Yan and Wang* [1999] indicates a clear improvement (see Table 2). The Saastamoinen (SAAS) MF has an overall r.m.s. of 2.1 cm at 10°elevation angle (this function can not be used below this cut-off angle), more than four times worse than FCULa (see Table 2). It performs significantly worse for high latitude stations, reaching an r.m.s. of almost 6 cm for the Antarctic region. The MF developed by Yan and Wang (Y-W) performs better than Saastamoinen's but worse than either of our functions (see Figure 1). The new MFs are particularly better in low-latitude regions (especially North Africa and the Middle East), where

Y-W shows r.m.s. values near 3 cm, for $\epsilon = 10^\circ$ (the overall r.m.s. for this elevation angle is 1.5 cm – see Table 2). The higher r.m.s. values may reflect the limitations of the estimated coefficients, which are based on a standard atmosphere model.

In order to compare the new MFs against the Marini-Murray (M-M) model we have adopted the Saastamoinen ZD model [*Saastamoinen,* 1973, 107, p. 32] for combination with FCULa (the full model is named **FCULz** for discussion purposes). As we can see in Table 3, the ZD models by Saastamoinen and Marini-Murray have virtually the same accuracy (and will not therefore bias our comparison). We have adopted the Saastamoinen ZD model, as his formulation is much simpler and requires less input data (note that both models introduce a slight bias in ZD prediction). The results of this comparison show an overall improvement at the few millimetre level, for $\epsilon = 10^\circ$, as shown in Figure 1. This improvement is significantly larger for lower elevation angles, proving that the new MFs are better than the one embebbed in the M-M model.

In order to confirm the higher accuracy of the new MFs, we have analyzed two years (1999-2000) of SLR data (LAGEOS and LAGEOS 2) with both FCULz and M-M, with an elevation angle cut off set to 10°, to avoid the introduction of any bias in the solution with M-M (details of this analysis are given in a forthcoming paper). Even though the number of ranges taken below 20°tends to be too small to make any large difference, the improvement due to the use of the new MFs is evident in both the estimated station heights and the adjusted tropospheric ZD biases. For the thirty sites that were present in these solutions, the average height adjustment showed a 2% reduction in the mean and an even more significant 8% reduction in variance. At the same time, the proper apportioning of model error resulted in an average increase of 7% for the ZD biases with an insignificant variance increase of only 0.8%. A simultaneous estimation of the terrestrial GM (which determines dynamically the global scale), resulted in statistically insignificant changes at the 0.04 ppb level, indicating a robust definition of global scale from SLR which is practically impervious to atmospheric correction errors.

Acknowledgments. E. C. Pavlis gratefully acknowledges partial support of this project from NASA's Cooperative Agreement NCC5-339. Radiosonde data were kindly provided by the British Atmospheric Data Center (BADC). The ray-trace software was developed by James Davis, Thomas Herring, and Arthur Niell. Figure 1 was produced using the Generic Mapping Tools software [Wessel and Smith, 1995]. We thank Arthur Niell and an anonymous reviewer for comments on the manuscript.

References

Ciddor, P. E., Refractive index of air: New equations for the visible and near infrared, *Applied Optics, 35,* 1566–1573, 1996.

Ciddor, P. E., and R. J. Hill, Refractive index of air. 2. Group index, *Applied Optics, 38,* 1663-1667, 1999.

Dutton, J. A., *The Ceaseless Wind: An Introduction to the Theory of Atmospheric Motion,* Dover Publications, New York, 1986.

International Union of Geodesy and Geophysics (IUGG), Resolution 3 of the International Association of Geodesy, *Comptes Rendus of the XXII General Assembly*, 19-30 July 1999, Birmingham, 110-111, 1999.

Marini, J. W., Correction of satellite tracking data for an arbitrary tropospheric profile, *Radio Sci., 7,* 223-231, 1972.

Marini, J. W., and C. W. Murray, Correction of laser range tracking data for atmospheric refraction at elevations above 10 degrees. NASA-TM-X-70555, Goddard Space Flight Center, Greenbelt, Md., 1973.

McCarthy, D. D., IERS Conventions, *IERS Technical Note 21,* Central Bureau of IERS, Observatoire de Paris, Paris, 1996.

Mendes, V. B., *Modeling the Neutral-atmosphere Propagation Delay in Radiometric Space Techniques*, Ph.D. dissertation, Department of Geodesy and Geomatics Engineering Tech. Rep. No. 199, University of New Brunswick, Fredericton, New Brunswick, Canada, 1999.

Niell, A. E., Global mapping functions for the atmosphere delay at radio wavelengths, *J. Geophys. Res., 101,* 3227-3246, 1996.

Saastamoinen, J., Contributions to the theory of atmospheric refraction, In three parts, *Bulletin Géodésique, 105,* 279-298, *106,* 383-397, *107,* 13-34, 1973.

Wessel, P., and W. H. Smith, New version of the Generic Mapping Tools, *Eos Trans. AGU, 76,* 329, 1995.

Yan, H., and G. Wang, New consideration of atmospheric refraction in laser ranging data, *Mon. Not. R. Astron. Soc., 307,* 605-610, 1999.

R. B. Langley, Geodetic Research Laboratory, Department of Geodesy and Geomatics Engineering, University of New Brunswick, Fredericton, N.B. E3B 5A3, Canada (lang@unb.ca)

V. B. Mendes, Departamento de Matemática, Faculdade de Ciências da Universidade de Lisboa, 1749-016 Lisboa, Portugal (vmendes@fc.ul.pt)

D. E. Pavlis, Raytheon Information Technology and Science Services and NASA Goddard 926, Greenbelt, MD 20771, USA (dpavlis@magus.stx.com)

E. C. Pavlis, Joint Center for Earth Systems Technology, University of Maryland Baltimore County and NASA Goddard 926, Greenbelt, MD 20771, USA (epavlis@helmert.gsfc.nasa.gov)

G. Prates, Escola Superior de Tecnologia da Universidade do Algarve, Faro, Portugal (gprates@ualg.pt)

(Received _____.)

Table 1. Coefficients (a_{ij}) for FCULa and FCULb MFs (see Equations (5) and (6)).

a_{ij}	FCULa	FCULb
a_{10}	$(12100.8\pm1.9)\times10^{-7}$	$(11613.1\pm1.6)\times10^{-7}$
a_{11}	$(1729.5\pm4.3)\times10^{-9}$	$(-933.8\pm9.7)\times10^{-8}$
a_{12}	$(319.1\pm3.1)\times10^{-7}$	$(-595.8\pm4.1)\times10^{-11}$
a_{13}	$(-1847.8\pm6.5)\times10^{-11}$	$(-2462.7\pm6.8)\times10^{-11}$
a_{14}		$(1286.4\pm2.2)\times10^{-7}$
a_{20}	$(30496.5\pm6.6)\times10^{-7}$	$(29815.1\pm4.5)\times10^{-7}$
a_{21}	$(234.6\pm1.5)\times10^{-8}$	$(-56.9\pm2.7)\times10^{-7}$
a_{22}	$(-103.5\pm1.1)\times10^{-6}$	$(-165.5\pm1.1)\times10^{-10}$
a_{23}	$(-185.6\pm2.2)\times10^{-10}$	$(-272.5\pm1.9)\times10^{-10}$
a_{24}		$(302.0\pm5.9)\times10^{-7}$
a_{30}	$(6877.7\pm1.2)\times10^{-5}$	$(68183.9\pm9.1)\times10^{-6}$
a_{31}	$(197.2\pm2.8)\times10^{-7}$	$(93.5\pm5.4)\times10^{-6}$
a_{32}	$(-345.8\pm2.0)\times10^{-5}$	$(-239.4\pm2.3)\times10^{-9}$
a_{33}	$(106.0\pm4.2)\times10^{-9}$	$(30.4\pm3.8)\times10^{-9}$
a_{34}		$(-230.8\pm1.2)\times10^{-5}$

Table 2. Statistics for mapping functions and full refraction models (in bold). See text for details.

ϵ (°)	Model	mean (cm)	std (cm)	r.m.s. (cm)	max (cm)
	M-M	0.76	0.26	0.80	1.26
	FCULa	-0.03	0.14	0.14	0.32
	FCULb	-0.03	0.16	0.16	0.35
15°	**FCULz**	0.46	0.23	0.51	0.90
	SAAS	-0.01	0.63	0.63	1.69
	Y-W	-1.09	0.38	1.16	1.74
	M-M	0.93	0.61	1.11	2.11
	FCULa	-0.03	0.44	0.44	0.93
	FCULb	-0.02	0.49	0.49	1.03
10°	**FCULz**	0.66	0.48	0.82	1.53
	SAAS	-0.48	2.03	2.08	5.83
	Y-W	-1.06	1.06	1.50	2.94
	M-M	-7.13	2.20	7.37	9.83
	FCULa	0.10	1.59	1.60	3.06
	FCULb	0.13	1.82	1.84	3.60
6°	**FCULz**	1.06	1.61	1.92	4.15
	SAAS	–	–	–	–
	Y-W	0.37	3.52	3.54	9.66

Table 3. Statistics for the Marini-Murray and Saastamoinen ZD models (total zenith delay). See text for details.

ϵ (°)	Model	mean (cm)	std (cm)	r.m.s. (cm)	max (cm)
90°	M-M	1.19	0.58	1.33	2.00
90°	SAAS	1.18	0.56	1.30	2.04

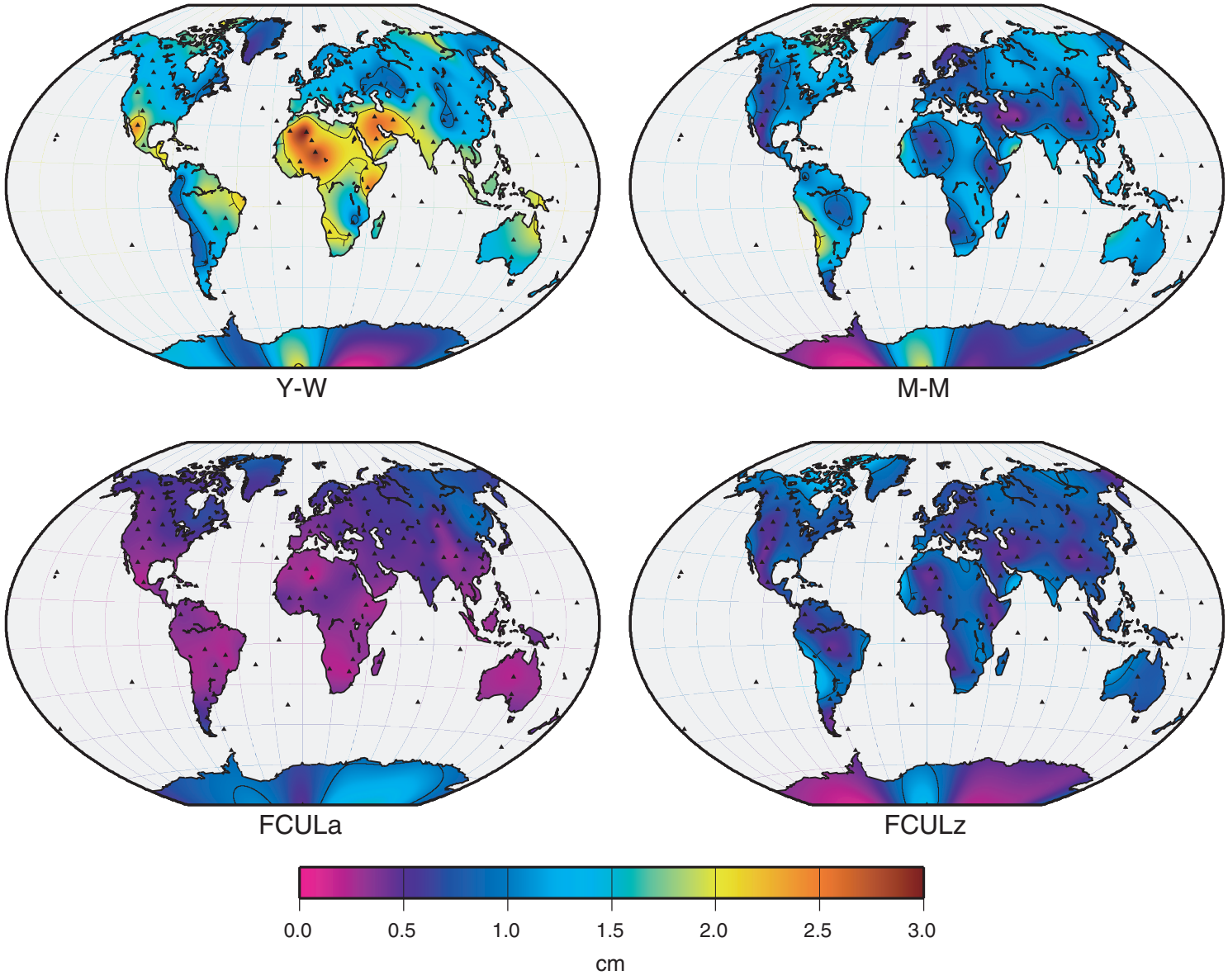
Y-W
M-M
FCULa
FCULz
0.0
0.5
1.0
1.5
2.0
2.5
3.0
cm